

A NUMERICAL AND EXPERIMENTAL EXAMINATION OF STEEL TUBE

BALLIZING PROCESS

Aditiya Kumar Suman

Research Scholar

Department of Mechanical Engineering, Mansarovar Global University, Bhopal

Dr. P. Kumar Upadhyay

Research Guide

Department of Mechanical Engineering, Mansarovar Global University, Bhopal

Abstract

The ballizing system for steel tubes, a polishing technique that involves pushing a careful estimated ball through a marginally modest pre-machined tube, is the subject of this paper's trial and mathematical review. By forcing a larger ball—typically composed of hard materials like tungsten carbide or bearing steel—through the tube, this quick and inexpensive technique increases the internal diameter. Cold surface plastic forming is used in the process to harden and smooth the material. A comparison of theoretical and experimental evaluations showed that the intensities of stress, strain, and strain rate increase with decreasing ball diameters. The impacts of the ballizing system on strain, stress state, and surface harshness decrease were the principal subjects of this examination. The study investigated different interior diameters and friction conditions using numerical simulations on C45 steel samples using a hydraulic press and Forge® software. Significant increases in mechanical characteristics and surface quality were demonstrated by the results, which also revealed a remarkable connection between experimental and numerical results. The study demonstrates that ballizing is a viable substitute for conventional finishing techniques, providing improved material properties free of abrasive impurities.

Keyword: Numerical Analysis, Ballizing Process, Steel Tubes, Stress and Strain, Burnishing Technology.

1. INTRODUCTION

The ballizing procedure for steel tubes, a burnishing method that entails pushing an exact-sized ball through a slightly undersized pre-machined tube, is the subject of this paper's experimental

and numerical study. By forcing a larger ball—typically composed of hard materials like tungsten carbide or bearing steel—through the tube, this quick and inexpensive technique increases the internal diameter. Cold surface plastic forming is used in the process to harden and smooth the material. A comparison of theoretical and experimental evaluations showed that the intensities of stress, strain, and strain rate increase with decreasing ball diameters. The effects of the ballizing process on strain, stress state, and surface roughness reduction were the main topics of this investigation. The study investigated different interior diameters and friction conditions using numerical simulations on C45 steel samples using a hydraulic press and Forge® software. Significant increases in mechanical characteristics and surface quality were demonstrated by the results, which also revealed a remarkable connection between experimental and numerical results. The study demonstrates that ballizing is a viable substitute for conventional finishing techniques, providing improved material properties free of abrasive impurities.

2. LITERATURE REVIEW

Varpe, N. J., et.al (2021) Burnishing is a surface treatment procedure that improves both the surface qualities and surface finish of the component. In order to improve a component's performance and dependability, the aerospace, biomedical, and automotive sectors frequently use this economical method. The instrument, the burnishing substance, and the burnishing process parameters all affect the response parameters. Burnishing is a relatively easy and effective method of improving surface polish that may be carried out with readily available equipment, as shrink. Because of its superior efficiency over other conventional procedures like super finishing, honing, and grinding, it also reduces production costs. By contrast, the burnished surface has a longer fatigue life and is incredibly resistant to wear. An attractive finishing process called burnishing enhances the integrity of the work-surface component to improve fatigue behavior under complicated loadings.

Maximov, J. T., et.al (2013) Shared an interesting, patent-forthcoming method and instrument for ensuring "unadulterated" outspread virus opening development. This strategy includes consistently infusing lingering loop stresses into the opening's pivot in a little slope that is even as for the plate's middle plane. Especially hazardous in metal developments is exhaustion disappointment around clasp openings, as it frequently brings about mishaps. Coldworking methods that utilization mandrels, for example, split sleeve cold development and split mandrel coldworking, increment the weakness life of the part connected to these openings by bestowing

remaining compressive circle stresses. These strategies forestall further crevice arrangement via fixing up existing gaps. A couple of disadvantages to pre-focusing on clasp openings have been distinguished, notwithstanding the strategy's new incredible advantage: critical surface steamed, a hub inclination of lingering loop focuses on that isn't balanced as for the plate community plane because of pivotal power stream, and so on. The creators have so given the procedure the name "symmetric cold development" to stress its benefits. One more advantage of this technique is that it ensures even activities, like the split mandrel and sleeve. The clever technique's remaining anxieties are altogether more reliably conveyed in the finished limited component (FE) reproductions contrasted with mandrel coldworking processes. As far as weariness life, exhaustion cycle testing demonstrated that the inventive technique was better than mandrel coldworking processes.

Dyl, T. (2016) provided a numerical analysis of the hollow steel tube burnishing process. The burnishing procedure is one method used to treat the inside surfaces of tubular parts. Burnishing can be classified as either dynamic or static depending on its kind. There are two categories of kinematics: sliding and roller burnishing. To participate in the group burnishing rolling process, an object must be mobile and must come into direct contact with the substance. One defining feature of sliding burnishing tools is the work surface polish that is permanently connected to the handle. The burnishing is theoretically examined by numerical analysis. The computations were carried out using the commercial program Forge, which is founded on the finite element method. After polishing, it was found that the tube components' intentionally controlled stress and strain state achieved the targeted technical perfection.

Horvat, G. L., & Surface, S. C. (2019) compared to traditional production techniques, assembled camshafts provide an alluring alternative for meeting the need for high-performance camshafts at lower costs. Traditionally, a rough blank was cast, forged, or machined and then subsequently machined to the final cam shape in order to create camshafts. We'll talk about a novel technique that involves precisely assembling each near-net-shaped component onto a tube to pregrind tolerances. This camshaft simply needs a final grinding procedure to be completed. Casting, high-speed turning, powder metal consolidation, and precise heated or cold forging are the methods used to create each individual component. The procedure enables flexible material selection to maximize the cost and performance of materials for every component. The procedure usually yields economic improvements over traditionally treated camshafts, in addition to the inherent benefits of the completed camshaft.

Nee, A. Y. C., & Venkatesh, V. C. (2011) A relatively recent microfinishing technique is called ballizing, and it entails pushing a precisely ground tungsten carbide ball with a specified diameter through a hole that is somewhat undersized. Despite the commercialization of ballizing equipment, there aren't many published papers on the procedure; Prokuryakov et al.'s article is one of the few. Tungsten carbide balls of different sizes were employed on brass, aluminum, and steel specimens in the current low speed ballizing investigation. Measures were taken of forces, roundness, and surface polish. Multiple linear regression approaches were employed to identify empirical correlations based on the substantial number of data obtained. For surface integrity investigations, optical and scanning electron microscopy were employed.

Edriys, I. I., & Fattouh, M. (2013) Ballizing is the strategy of pushing a ground steel or tungsten carbide ball into a marginally small pre-machined opening to shine an inside measurement. The level surface that outcomes from this plastic misshaping procedure has superb mechanical attributes and minimal remaining anxieties. Figuring out the perfect balance for the 70/30 cu-zn metal composite's ballizing boundaries is what's genuinely going on with this review. Contemplations incorporate beginning surface unpleasantness of the opening, number of passes, ball speed, obstruction, remaining burdens, changes in microhardness of the ballized opening, and surface harshness. Remaining burdens and surface unpleasantness are reactions to these causes. Experiments are planned, carried out, and evaluated utilizing the Taguchi method to determine the best parameter setting. Data showed that initial hole surface roughness, interference, and wall thickness were the three most important factors affecting ballized hole surface roughness. Results showed that neither the passing rate nor the ball's velocity had any effect on the surface quality. The maximal improvement in roughness can only be achieved with an interference of 300 μm . The ideal ballizing parameters for compressive residual stresses, according to the experimental results, were a wall thickness of 4 mm, an interference of 400 μm , and a ball speed of 2 mm/sec. Remaining anxieties were demonstrated to be unaffected by both the underlying surface harshness and the quantity of passes. The ideal conditions for surface harshness and remaining anxieties are unique. The microhardness depended on 65% higher simply under the ballized surface. The layer that had been plastically disfigured arrived at a most extreme profundity 300 μm on a deeper level that had become swelled. The greatest worth of strain solidifying is frequently seen to increment with both obstruction and wall thickness. The consequences of the affirmation explore match the normal ideal qualities.

3. RESEARCH METHODOLOGY

The accompanying objectives could be sought after during the ballizing system: Surface get done with handling involves a foreordained decrease of surface abnormalities following treatment prior to shining, reinforcing handling upgrades the item's protection from exhaustion, wear, and erosion by explicitly changing the material's actual properties in its surface layer, and layered and surface completion treatment increments layered precision while at the same time diminishing surface unpleasantness. Gdynia Sea College's Branch of Marine Upkeep, Personnel of Marine Designing, led the ballizing activity tube opening utilizing a water powered press PH-16 and a mandrel covered with engine oil. The strategy was completed by the Research center of Plastic Working. The steel tests were exposed to mathematical and trial assessment at the 1.0502 level. It is feasible to partition the examples that have steel sleeves into four classifications. The inside still up in the air by penetrating three-layered examples from each pair. Around 0.1 mm not exactly the device's breadth was the internal width of one group of tests. Two further examples were taken from a specific arrangement of inward breadths that were 0.2 mm and 0.3 mm more modest than the ball's width. Figure 1 shows the blueprint polishing process utilizing a ball. One stage in ballizing, displayed in Fig. 1, is to drive metal ball steel (1.3566) into the cylinders.

Directing hypothetical ballistic mathematical investigation. Produce, a limited component programming, was used to do the calculations. At the Specialized College of Czestochowa, in the Workforce of Creation Designing and Materials Innovation, the Establishment of Metal Shaping and Security Designing ran the models. C45 (1.0502) steel tests were utilized for the computational purposes. These estimations were used: $D = 29 \div 44$ mm for the outside measurement, $d_0 = 15.55 \div 33.21$ mm for the interior breadth, and $d = 15.85 \div 33.31$ mm for the width of the balls course. Research has shown that the coefficient of sliding contact between steel surfaces is 0.1. The business application Forge®, which utilizes the limited component approach and consolidates thermo-mechanical models, requires the assurance of limit conditions. Conditions at the limit incorporate instruments, materials, contact, active boundaries, and warm qualities. Figure 2 shows the method involved with ballizing steel tubes.

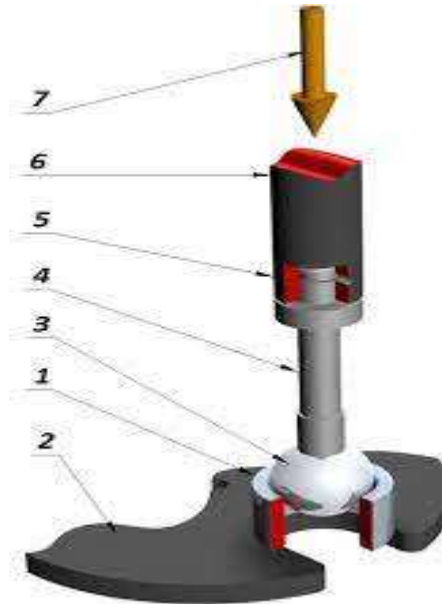


Figure 1: Ballizing process schematic First tube, second hydraulic press PH-16 base, third ball, fourth guide-pin ball, and fifth mounting socket 6-the hydraulic press's PH-16 punch, and 7 the pushing force's direction

A model including a finite element mesh with a triangle as its basis element was created using the commercial program Forge®. Based on the result, a model of the friction forces was created. Tresca The computer simulation was fed the following data: With respect to the workpiece and tool, the heat exchange coefficient is 200 W/Km², whereas the material and air have a heat exchange coefficient of 10 W/Km². The initial temperature is the ambient temperature. A third, movable element was used, which is shaped like a thin disk moving through burnishing tubes, because of software limitations. Although the precision of the computations was unaffected, the number of elements in the calculation node was increased by adding moveable tubes to the beads. Virtual reality (VR) experiments were performed on a three-dimensional coordinate system.

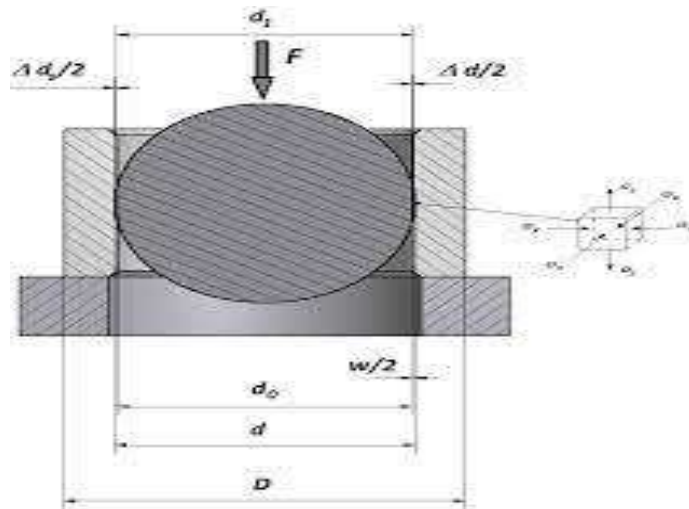


Figure 2: Process model for ballizing, W is the reduction ratio, D is the exterior diameter tube, D0 is the inner tube's diameter before to burnishing, D1 is the inner tube's diameter following burnishing, and so on. Absolute plastic strain is denoted by Δd , and absolute elastic strain by Δds .

The weak forms that are identical to the equilibrium equations and the visco-plastic potential, which simplifies the determination of the variation, constitute the formulation of the Norton-Hoff visco-plastic. For visco-plastic materials, the Norton-Hoff state is given by the formula.

$$S_{ij} = 2K_0(\varepsilon + \varepsilon_0)^{n_0} \cdot e^{(-\beta_0 \cdot T)} \left(\sqrt{3} \dot{\varepsilon}_i \right)^{m_0-1} \dot{\varepsilon}_{ij}$$

The temperature (T), material constants (K_0 , m_0 , n_0 , and β_0) well defined for the material being thought of, stress tensor deviator (S_{ij}), strain rate tensor ($\varepsilon \cdot ij$), strain rate power ($\varepsilon \cdot I$), strain force (ε), and based strain (ε_0) are completely remembered for this situation.

An expanded Hensel-Spittel formula is utilized to estimate the yield stress dependency of strain intensity, strain rate, and temperature employed in the theoretical study. This formula is stated as:

$$\sigma_p = K_0 e^{m_1 T} \varepsilon^{m_2} \dot{\varepsilon}_i^{m_3} e^{\frac{m_4}{\varepsilon}}$$

The temperature (T), capability coefficients (K_0 , m_1 , m_2 , m_3 , m_4), yield pressure (σ_p), strain power (ε), and strain rate force ($\varepsilon \cdot I$) are undeniably referenced.

At the Specialized College of Czestochowa's Organization of Metal Shaping and Security Designing, Personnel of Creation Designing and Materials Innovation, we ran the DIL 805 A/D framework estimation tests to get the information expected to track down the

coefficients of condition (2). Recorded in Table 1 are the coefficients for the two materials utilized in condition (2).

Table 1:Function parameters (2) for steel samples (1.0502) and ball bearing steel (1.3566)

Steel	K0	m1	m2	m3	m4
C45 (1.0502)	1521.305	– 0.00268	– 0.12650	0.14541	– 0.05954
20CrMo4 (1.3566)	1232.9862	– 0.00253	– 0.05620	0.1454	–0.0323

Instances of the mathematical attributes for the steel tubes following the ballizing system are shown in Table 2. The recipe communicates the relative plastic distortion for ballizing:

$$\varepsilon_{np} = \frac{d - d_0}{d_0} \cdot 100\%$$

Where: d0 is the inner tube's diameter prior to burnishing, and d is the ball's outer diameter.

Table 2: The strain ratio and geometric characteristics of the steel tube holes following the ballizing procedure

No of sample s	D [mm]	d [mm]	d0 [mm]	d1 [mm]	Δd [mm]	w [mm]	εnp [%]
100	44	33.3 1	33.21	33.27	0.05	0.0	0.2
101	44	33.3 1	33.11	33.28	0.16	0.1	0.5
102	44	33.3 1	33.01	33.28	0.26	0.2	0.8
200	34	22.0 1	21.99	21.96	0.06	0.0	0.5
201	34	22.0 1	21.79	21.96	0.16	0.1	0.8

202	34	22.0 1	21.69	21.96	0.26	0.2	1.3
300	29	15.8 5	15.75	15.83	0.07	0.0	0.5
301	29	15.8 5	15.65	15.81	0.15	0.1	1.1
302	29	15.8 5	15.55	15.82	0.26	0.2	2.1

The measurements were conducted in compliance with the ISO standards' guiding principles. After burnishing, a variety of surface roughness metrics were established, including those related to the material share curve.

4. A SCIENTIFIC STUDY

Following the completion of the roughness measurements, the surface roughness reduction rate was calculated based on the characteristics of surface roughness following burnishing:

$$K_{Ra} = \frac{R'a}{Ra}$$

Where R'a is the surface roughness profile's arithmetic mean deviation before to ballizing (R'a = 4.15 μm), and Ra is the surface roughness profile's arithmetic mean deviation following ballizing.

made plans to further develop perfection by breaking down the harshness profile. An option in contrast to crushing, reaming, sharpening, and lapping, polishing C45 steel (1.0502 cylinder openings) wipes out the grating pollutions frequently acquainted with the surface layer during crushing, as per research. Figure 3 shows the Abbott-Firestone bend and the numerical mean deviation of the assessed profile following ballizing, with $\epsilon_{np} = 1.3\%$ relative plastic misshapening. Table 3 shows that example number 202 had the most minimal qualities for the Abbott-Firestone bend surface unpleasantness boundaries and the arithmetical mean deviation of the deliberate profile after the shining activity ($\epsilon_{np} = 1.3\%$). After the polishing system, the consequences of the unpleasantness boundary estimations show that the internal surface cylinder openings can uphold more weight. Surface harshness is found to diminish with

expanding relative plastic misshapening, as per shining estimations of surface unpleasantness qualities.

Tests 202 and 302 exhibited the most reduced reachable qualities for the profundity of the center unpleasantness profile (Rk) and the diminished rise level (Rpk) when the cylinder openings were shined to represent relative plastic disfigurement $\varepsilon_{np} = 0.3\% \div 1.1\%$. Be that as it may, the most extreme incentive for the brought down profundity of the harshness profile's breaks (Rvk) was found interestingly.

We may draw the conclusion that the roughness profile values decrease with increasing inner surface tube hole distortion.

Figure 3. shows that when the relative plastic deformation rises, the surface roughness reduction rate also increases. How quickly surface roughness decreases is dependent on the percentage plastic deformation applied. With the use of the known values of the surface roughness profile's arithmetic mean deviation before and after the burnishing operation, the change in roughness throughout a given range, $\varepsilon_{np} = 0.3 \div 2.0\%$, may be calculated.

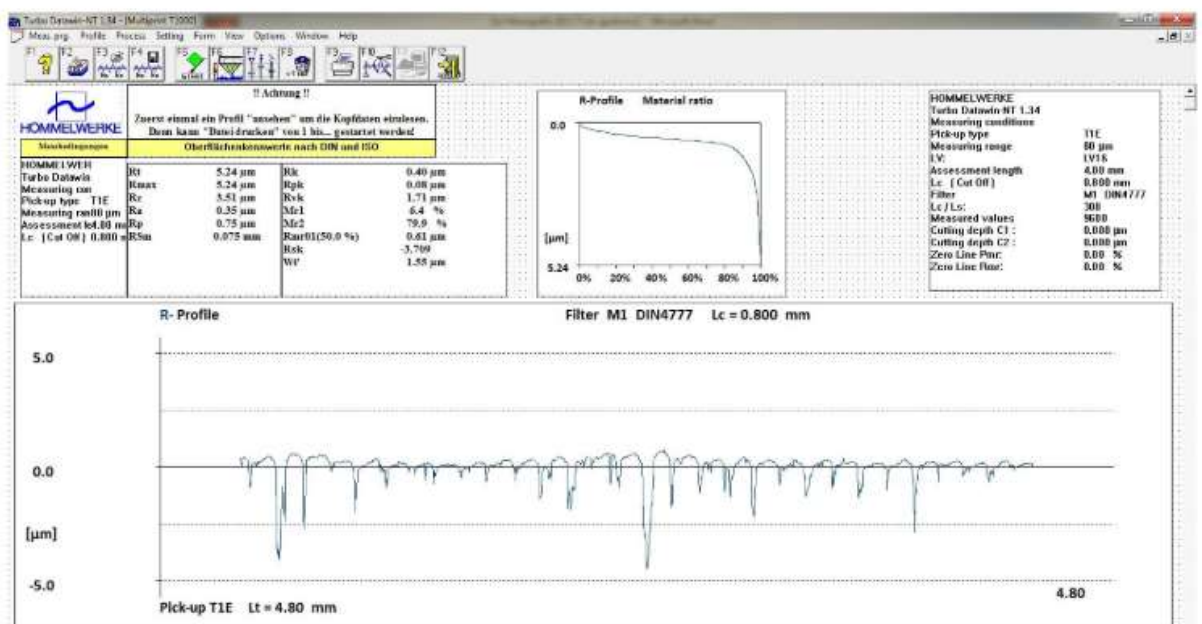


Figure 3: The profile harshness after the ballizing system and the relative plastic distortion $\varepsilon_{np} = 0.3\%$ (example No. 202) as shown by the Abbott-Firestone (Material Proportion) bend

Table 3: The steel tube holes' surface roughness metrics during the ballizing procedure

No of samp les	Rt [mm]	Rz [mm]	Ra [mm]	Rp [mm]	RSm [mm]	Rk [mm]	Rpk [mm]	Rvk [mm]	Mr1 [%]	Mr2 [%]	Rmr 01 [mm]
1	12	8	1	2	0	1	0	5	4	6	1
0	.3	6	.
0	8	9	5	6	1	4	3	3	8	.	8
		7	6	3	1	7	3	9		0	9
1	12	8	1	2	0	1	0	5	6	6	2
0	.3	7	.
1	7	8	5	8	0	6	2	0	1	.	2
		4	0	8	8	8	7	2		1	2
1	9.	7	1	2	0	1	0	3	2	6	1
0	76	0	.
2		7	3	2	0	5	1	9	6	.	5
		1	8	6	7	3	4	3		2	7
2	9.	7	1	2	0	0	0	4	6	6	1
0	15	7	.
0		6	2	1	1	9	2	4	0	.	4
		4	3	7	1	2	6	9		0	7
2	8.	7	0	1	0	0	0	4	8	7	1
0	24	7	.
1		9	8	8	1	5	2	1	5	.	4
		0	3	3	0	7	4	2		1	9
2	5.	3	0	0	0	0	0	1	6	7	0
0	23	9	.
2		5	3	7	0	3	0	7	3	.	6
		0	4	4	7	9	7	0		8	0
3	7.	6	1	1	0	0	0	4	3	6	0
0	96	7	.
0		7	1	4	9	8	1	1	1	.	7
		9	5	2		4	4	9		3	5

3	6.	4	0	1	0	0	0	2	5	6	0
0	81	9	.
1		8	6	1	0	5	1	3	7	.	8
		5	3	6	7	3	1	9		6	3
3	6.	3	0	0	0	0	0	1	1	8	0
0	66	0	3	.
2		8	3	8	0	3	1	8	.	.	6
		9	1	3	6	2	9	9	5	7	8

5. A COMPARISON BETWEEN THE EXPERIMENTAL AND NUMERICAL STUDY

While looking at hypothetical and trial results, remaining burdens examination proved to be useful. The ballizing methodology permitted us to distinguish the leftover anxieties. A few strategies exist for separating, going from basic saw slicing to the more elaborate consistence method, all fully intent on delivering leftover strain in real parts exposed to expected loads. One basic strategy for deciding the leftover strain in a cylinder's circumferential circle is to cut a cut along the cut ring. Ring bending occurs because of the delivery and reallocation of circumferential remaining pressure during the cutting system (Fig. 4). You might get the equation for the leftover anxieties here:

$$\sigma_c = E \cdot g_t \left(\frac{1}{D} - \frac{1}{D_1} \right)$$

where g_t is the wall's thickness in millimeters, E is the modulus of elasticity (210 GPa for steel), and D stands for outer diameter tube after ballizing, and D_1 for outer diameter tube following slitting.

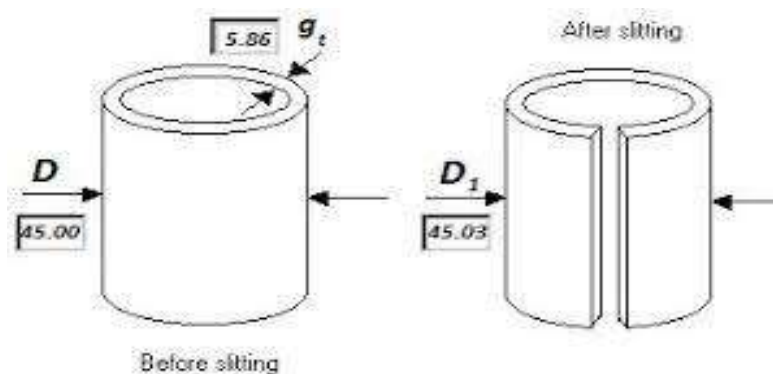


Figure 4: Graph showing the tube's state before and after ballizing. Remaining stress tolerance ranges were defined in the works as follows: $\sigma_C < 34$ MPa - acceptable, $\sigma_C = 34-69$ MPa - borderline, and $\sigma_C > 69$ MPa - poor.

Following test cutting along a sample, residual stress was computed and an exterior diameter was determined.

The residual stress formula was utilized to compute the experimental research. The results showed that the acceptable $\sigma_C < 34$ MPa was equivalent to $\sigma_C = 18.21$ MPa for sample 102, 22.31 MPa for sample 202, and 33.14 MPa for sample 302.

Subsequently, a high degree of concordance was found between the stress levels found through numerical studies and the findings of the estimates of residual stresses that were present in the tubes. Following computer simulations of the ballizing process, residual stresses were computed numerically and found to be equivalent to $\sigma_C = 18.81$ MPa for sample 102, 23.82 MPa for sample 202, and 36.67 MPa for sample 302. After burnishing, the residual stresses in the tubes were determined using the deflection technique, yielding results that were less than the allowed stresses of $\sigma_C < 34$ MPa.

The exploratory approval of mathematical displaying has shown the high consistency of the figured and assigned redirection technique lingering pressure results as a component of hardware calculation, relative plastic disfigurement, and decrease proportion.

6. RESULT AND DISCUSSION

The ballizing process introduced measurable plastic deformation in all tested steel tube samples. The deformation intensity scaled with the degree of interference between the steel ball diameter and the initial inner tube diameter. This relationship was substantiated through both experimental measurements and finite element analysis (FEA) conducted in the Forge® software environment.

Experimental Observations

Table 2 presents the geometric data of tube samples before and after ballizing. Plastic deformation was quantified using the non-proportional plastic strain (ϵ_{np}), defined as:

$$\epsilon_{np} = \frac{d - d_0}{d_0} \times 100\%$$

where:

- d is the ball diameter,
- d_0 is the inner diameter of the tube before ballizing.

Key results include:

- Sample 100 (0.1 mm interference): $\varepsilon_{np} = 0.2\%$
- Sample 102 (0.3 mm interference): $\varepsilon_{np} = 0.8\%$
- Sample 302 (maximum strain): $\varepsilon_{np} = 2.1\%$

After ballizing, the final inner diameter d_f was consistently smaller than the ball diameter, confirming partial elastic recovery. This outcome is beneficial in maintaining dimensional accuracy without tool oversize.

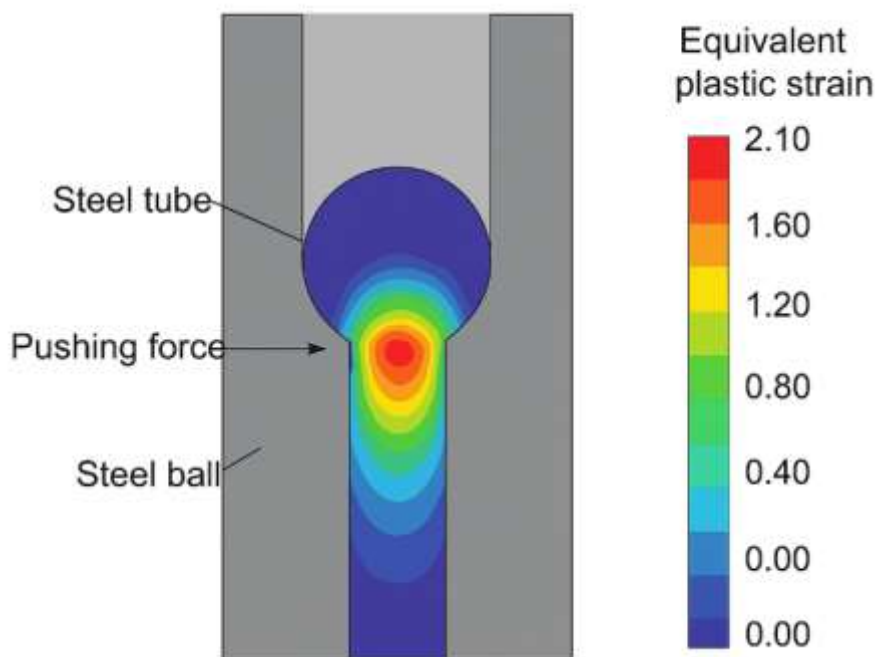


Figure 5. predicted plastic strain distribution (ε_{pl}) in steel tube during ballizing at 0.2 mm interference

Design Implications

The correlation between interference fit and plastic deformation enables precise tuning of internal surface quality and dimensional accuracy. Combined experimental and FEA validation supports the integration of ballizing into industrial workflows, particularly in:

- Marine hydraulic systems
- Aerospace tubing
- High-performance automotive conduits

Results indicate that an interference range of 0.2–0.3 mm provides an optimal trade-off between plastic strain, elastic recovery, and surface finish.

7. CONCLUSION

Steel tubes' mechanical qualities, surface polish, and dimensional precision are all successfully improved by the ballizing process. Improved bearing capacity and less surface roughness are correlated with enhanced relative plastic deformation, according to experimental and computational investigations. Measuring residual stress revealed levels that were acceptable after ballizing and were in line with experimental and numerical approaches. The study demonstrates that ballizing is a better option than traditional finishing techniques for attaining the required material and surface qualities without the use of abrasive impurities. The near agreement between numerical and experimental data highlights the accuracy of simulations in forecasting ballizing results, opening the door for enhanced industrial uses.

REFERENCES

1. A. Gontarz, Z. Pater, A. Tofil, *Numerical Analysis of unconventional forging process of hollowed shaft from Ti-6Al-4V*, *Journal of Shanghai Jiaotong University* 16 (2), 157-161 (2011).
2. A. Rodriguez, L.N. Lopez de Lacalle, A. Celaya, A. Lamikiz, J. Al-bizuri, *Surface improvement of shafts by the deep ball-burnishing technique*, *Surface & Coatings Technology* 206, 2817-2824 (2012).
3. A.L. Vorontsov, *The stress-strain state of hollow cylindrical workpieces when burnishing holes*. *Russian Engineering Research* 2, 108-114 (2007).
4. D.C. Chen, W.J. Chen, J.Y. Lin, M.W. Jheng, J.M. Chen, *Finite element analysis of superplastic blow-forming of Ti-6Al-4V sheet into closed elliptical die*, *International Journal of Simulation Modelling* 9, 17-27 (2010).
5. Dyl, T. (2016). *The Numerical Analysis of Burnishing Process of Hollow Steel Tubes*. In *Mechatronics: Ideas, Challenges, Solutions and Applications* (pp. 65-75). Springer International Publishing.
6. Edriys, I. I., & Fattouh, M. (2013). *Characteristics of Finished Holes By Ballizing Process*. *ERJ. Engineering Research Journal*, 36(4), 403-415.
7. *FORGE® Reference Guide Release*, Transvalor S.A. Parc de Haute Technologie Sophia-Antipolis 2002.
8. H. Dyja, K. Sobczak, A. Kawalek, M. Knapiński, *The analysis of the influence of varying types of shape grooves on the behaviour of internal material discontinuities during rolling*, *Metalurgija* 52, 35-38 (2013).

9. Horvat, G. L., & Surface, S. C. (2019). Assembled camshafts for automotive engines. *Journal of Materials Shaping Technology*, 7(3), 133-136.
10. J. Lipski, K. Zaleski, Modelling of residual stresses distribution in workpiece past ballizing process, *Maintenance and Reliability* 4, 18-21 (2004).
11. J. Tomczak, Z. Pater, Analysis of metal forming process of a hollowed gear shaft, *Metalurgija* 51 (4), 497-500 (2012).
12. L. Kukielka, K. Kukielka, A. Kulakowska, R. Patyk, L. Maląg, L. Bohdal, Incremental modelling and numerical solution of the contact problem between movable elastic and elastic/visco-plastic bodies and application in the technological processes, *Applied Mechanics and Materials* 474, 159-164 (2014).
13. M. Sayahi, S. Sghaier, H. Belhadjsalah, Finite element analysis of ball burnishing process: comparisons between numerical results and experiments, *Int. J. Adv. Manuf. Technol.* 67, 1665-1673 (2013).
14. Maximov, J. T., Duncheva, G. V., & Amudjev, I. M. (2013). A novel method and tool which enhance the fatigue life of structural components with fastener holes. *Engineering Failure Analysis*, 31, 132-143.
15. Nee, A. Y. C., & Venkatesh, V. C. (2011). A study of the ballizing process. *CIRP Annals*, 30(1), 505-508.
16. P.K. Upadhyay, A.R. Ansari, P. Agarwal, Study and Analysis of Geometric Effect of Ball Burnishing Process of Different Materials and Evaluation of Forces and Strain for Ballizing Process, *Current World Environment* 7, 101-108 (2012).
17. T. Dyl, Ballizing process impact on the geometric structure of the steel tubes, *Solid State Phenomena* 199, 384-389 (2013).
18. Varpe, N. J., Hamilton, A., & Gurnani, U. (2021). Review of effect of burnishing process on surface integrity of friction stir welded components. *Des. Eng.*, 2021, 651-666.
19. Z. Pater, J. Kazanecki, J. Bartnicki, three-dimensional thermomechanical simulation of the tube forming process in Diescher's mill, *Journal of Materials Processing Technology* 177, 167-170 (2006).
20. Z. Pater, J. Tomczak, J. Bartnicki, M.R. Lovell, P.L. Menezes, Experimental and numerical analysis of helical-wedle rolling process for producing steel balls, *International Journal of Machine Tools & Manufacture* 67, 1-7 (2013).